Available online at www.sciencedirect.com

ScienceDirect

Ceramics International 39 (2013) 9599–9603

CERAMICS INTERNATIONAL

www.elsevier.com/locate/ceramint

Synthesis of composite $La_{1.67}Sr_{0.33}NiO_4$–YSZ for a potentiometric NOx sensor by microwave-assisted complex-gel auto-combustion

Ying Chen, Jian-Zhong Xiao*

School of Materials Science and Engineering, State Key Laboratory of Material Processing and Die & Mould Technology, Huazhong University of Science and Technology, Luoyu Rd 1037, Wuhan, Hubei 430074, PR China

Received 22 January 2013; received in revised form 11 April 2013; accepted 1 May 2013
Available online 27 May 2013

Abstract

This paper reports a facile microwave-assisted complex-gel auto-combustion method synthesis of $La_{1.67}Sr_{0.33}NiO_4$ and YSZ composite powders and their utilization for the fabrication of high performance potentiometric NOx sensors. The synthesized composite powders with different YSZ concentrations (5 wt%, 10 wt% and 20 wt%) were characterized using Fourier transformed infrared (FTIR) spectrum and X-ray diffraction (XRD). The gas sensing property of the composites to NO was tested at temperatures ranging from 400 °C to 600 °C. The sensor fabricated with 10 wt% YSZ addition composite sensing electrode exhibited the biggest response (about 27 mV for 700 ppm NO) at 400 °C. Moreover, the response time and recovery time were within 4–18 s and 6–35 s, respectively. The enhanced gas sensing performance of the sensor to NO may be attributed to the larger superficial area of triple phase boundary. This work demonstrated that the simply synthesized $La_{1.67}Sr_{0.33}NiO_4$ and YSZ composite powders can be effectively used for the fabrication of potentiometric NOx sensors.

Keywords: Pontentiometric NOx sensor; Auto-combustion synthesis; $La_{1.67}Sr_{0.33}NiO_4$; YSZ; Triple phase boundary

1. Introduction

Nitrogen oxides (NOx) are major air pollutants generated from the reaction of nitrogen and oxygen in air during combustion processes, such as in power plants and automotive engines [1,2]. In areas of high motor vehicle traffic, the amount of NOx emitted into the atmosphere can be quite significant resulting in smog and acid rain and the formation of tropospheric ozone. Controlling the emission of such gases and developing high-performance sensors for continuously monitoring these gases in the emission process and ambient atmosphere are urgently required. So far, lots of potentiometric, amperometric, and impedancemetric NOx sensors based on solid electrolyte have been examined and reported [3]. Among these NOx sensors, the mixed potential type sensor using oxide electrode has merits of a simple structure and sustainability in a hostile condition of exhaust gas. There have been many studies on mixed potential NOx sensor adopting various oxides such as perovskite, spinnel type oxide and cathode materials of solid oxide fuel cell for a sensing electrode [4–6].

$La_2NiO_{4+\delta}$ was a mixed conductor with the K_2NiF_4-type structure and has recently received much attention due to its promising properties for SOFC cathode and ceramic membrane for oxygen separation and partial oxidation of light hydrocarbon. $La_2NiO_{4+\delta}$ exhibits a tetragonal crystal structure with space group I4/mmm, which can be imagined as alternating LaO rock salt and $LaNiO_3$ perovskite layers along the z axis [7]. Interstitial oxygen can be accommodated in its crystalline structure, promoting the ionic conductivity [8,9], and the p-type electronic conductivity [10]. Sr doped La_2NiO_4 was found to exhibit high electronic conductivity, as well as thermal and mechanical stability, which promised cathodic properties [11], due to their relatively high oxygen diffusion and surface exchange coefficients [12,13]. The yttria-stabilized zirconia (YSZ) was most frequently used in SOFC and NOx sensor as an electrolyte. When yttria stabilized zirconia was added into electrode, the electrode could enhance electrocatalytic activity, while maintaining adequate amount of reaction sites, e.g. the triple phase boundary (TPB) [14]. In the present paper, we reported a facile microwave-assisted

*Corresponding author. Tel.: +86 27 13507182990.
E-mail address: jzxiao@mail.hust.edu.cn (J.-Z. Xiao).

0272-8842/$ - see front matter © 2013 Published by Elsevier Ltd and Techna Group S.r.l.
http://dx.doi.org/10.1016/j.ceramint.2013.05.080

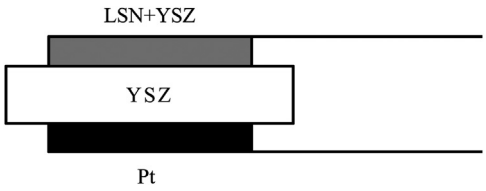

Fig. 1. Sensor configuration.

complex-gel auto-combustion synthesis method to synthesize $La_{1.67}Sr_{0.33}NiO_4$–YSZ composite powders, thereby increasing the length of the TPB. The as-prepared products were characterized by Fourier transformed infrared (FTIR) spectrum and X-ray diffraction (XRD). The gas sensing property of the fabricated NOx sensor based on the $La_{1.67}Sr_{0.33}NiO_4$–YSZ composites was investigated.

2. Experimental

2.1. Powder synthesis

A series of $La_{1.67}Sr_{0.33}NiO_4$–YSZ composite powders (YSZ=5 wt %, 10 wt %, and 20 wt %), in which the YSZ phase was intended to contain 5 mol% Y_2O_3, were synthesized by the microwave-assisted complex-gel auto-combustion synthesis method. Analytical grade lanthanum nitrate ($La(NO_3)_3 \cdot 6H_2O$), strontium nitrate ($Sr(NO_3)_2$), nickel nitrate ($Ni(NO_3)_2 \cdot 6H_2O$), zirconium nitrate ($Zr(NO_3)_4 \cdot 5H_2O$), yttrium nitrate ($Y(NO_3)_3 \cdot 6H_2O$), citric acid ($C_6H_8O_7 \cdot 6H_2O$ or CA), ethylene glycol ($C_2H_6O_2$ or EG) and NH_4OH were used as the starting materials. Firstly, stoichiometrical amounts of $La(NO_3)_2 \cdot 6H_2O$, $Sr(NO_3)_2$, $Ni(NO_3)_2 \cdot 6H_2O$, $Zr(NO_3)_4 \cdot 5H_2O$ and $Y(NO_3)_3 \cdot 6H_2O$ were dissolved in an appropriate amount of deionized water to form an aqueous solution, CA and EG were added into the solution, in which the molar ratios of CA to metal ions (CA:M) and EG to CA are 3:2 and 3:2, respectively. Then, aqueous ammonia of 28% was added dropwise into the solution until its pH reached 7. The solution was then continuously stirred at room temperature for 4 h for the formation of sol before it was heated at 80 °C for the removal of moisture to obtain the dried gel. The as-obtained gels were ignited after about 15 s of microwave irradiation in a microwave oven (Galanz: 2.45 GHz, 1180 W, 20 L). Once on ignition, the combustion took place fiercely, resulting in a fluffy combustion product, which was then subjected to an annealing treatment in air at 800 °C for 2 h. The FTIR spectra to characterize the fluffy powders were recorded on an IR-FFT spectrophotometer (VERTEX 70, Bruker) from 400 cm^{-1} to 4000 cm^{-1} by the KBr pellet method. The crystalline phase in the samples after annealing at 800 °C for 2 h was characterized by X-ray diffraction (XRD, Panalytical X'pert PRO MRD, Holland) using CuKα radiation.

2.2. Sensor fabrication

Tape cast YSZ disks with diameter of 16 mm were used for sensor fabrication. For fabrication of the sensing electrodes paste, $La_{1.67}Sr_{0.33}NiO_4$–YSZ composite powders were ball-milled with terpineol, ethylcellulose and span for 24 h. A square electrode (0.1×0.1 cm^2) of the $La_{1.67}Sr_{0.33}NiO_4$–YSZ mixture was printed on one side of a YSZ substrate and a Pt electrode (0.1×0.1 cm^2) was printed directly opposite to the $La_{1.67}Sr_{0.33}NiO_4$–YSZ electrode (Fig. 1). Thin Pt wires (0.1 mm in diameter) were connected to both electrodes. Finally, the sensors were sintered at 1000 °C for 2 h. Sintered electrode microstructures were observed by an environmental scanning electron microscope (ESEM, Quanta 200, FEI, Holland).

2.3. Testing parameters

Sensor experiments were conducted in a gas-flow apparatus (MPA-80). Gas environments were controlled using mass flow controllers (Beijing Seven Star Electronics Company). The total flow rate was set at a constant 200 ml min^{-1}. The fabricated sensors were exposed to 10% O_2 balanced by N_2. NO was exposed to the sensors in the following concentrations: 0, 100, 200, 500, and 700 ppm, holding each concentration for 150 s. The test temperatures were from 400 to 600 °C at 50 °C increments.

The voltage between the sensing and counter electrodes was measured during the step changes using an Electrochemical workstation (VearsaSTAT3, Princeton, USA). Both electrodes of the sensor were in the same gas atmosphere.

3. Results and discussion

3.1. Powder characterization

Fig. 2 shows the typical FTIR spectra for the pure citric acid and the auto-combustion product. When the composites contain 20 wt% YSZ, it can be seen that its major absorption bands appear at about 1595 cm^{-1}, 1384 cm^{-1} except for the ones in the high wave number region, which may be attributed to the asymmetric stretching vibrations and the symmetric ones of the carbonyls (COO^-) in the citrate carboxylate, respectively [15–17]. Furthermore, compared with the ones of pure citric acid, these characteristic absorption bands can be found to have a shift to lower frequency corresponding to absorption bands at 1736 and 1429 cm^{-1} and suggesting that the vibration states of ligands have changed due to their chelating with metal ions [18].

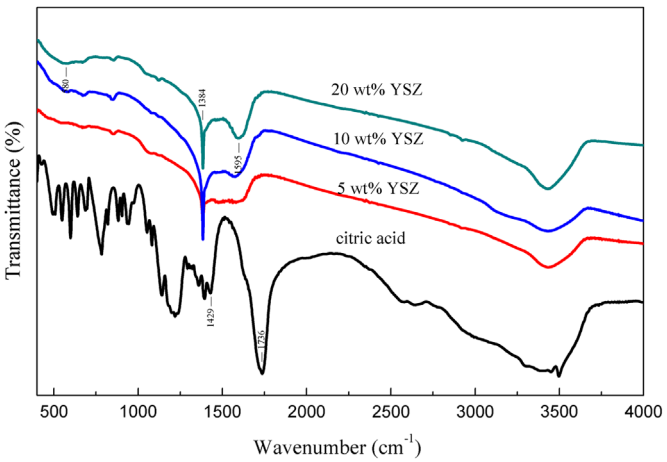

Fig. 2. FTIR spectra of pure citric acid and combustion product.

Consequently, it is postulated that the metal ions such as La^{3+}, Sr^{2+}, Ni^{2+}, Y^{3+} and Zr^{4+} are all well chelated into the complexes. The absorption bands for C–O groups [19] almost vanish; it reveals the fact that the organics in the dried gel have been burnt almost completely but there exist some unburnt substances, so a new absorption band appears around 673 cm^{-1}, which may be assigned to (La, Sr, Ni, Zr)–O bond's stretching vibration mode [20,21] and, therefore, implies the formation of oxides of La, Sr, Ni and Zr/Y. The composites that contain 5 wt% and 10 wt% YSZ are similar to the case of the 20 wt% YSZ addition.

Fig. 3 demonstrates the XRD patterns for the samples of the powders after annealing treatment. It can be seen that the samples with 5 wt% and 10 wt% YSZ addition are composed of $La_{1.67}Sr_{0.33}NiO_4$ and ZrO_2 cubic phases. But the formation of insulating pyrochlore phase ($La_2Zr_2O_7$) and the La_2NiO_4 phase can be observed when the composites contain 20 wt% YSZ.

3.2. Electrode microstructures

Scanning electron micrographs of the $La_{1.67}Sr_{0.33}NiO_4$–YSZ composite sensing electrode surfaces are shown in Fig. 4. As exhibited, the electrodes with different YSZ additions show a sheet structure. With the increasing of YSZ addition, the particle size of the composites becomes bigger.

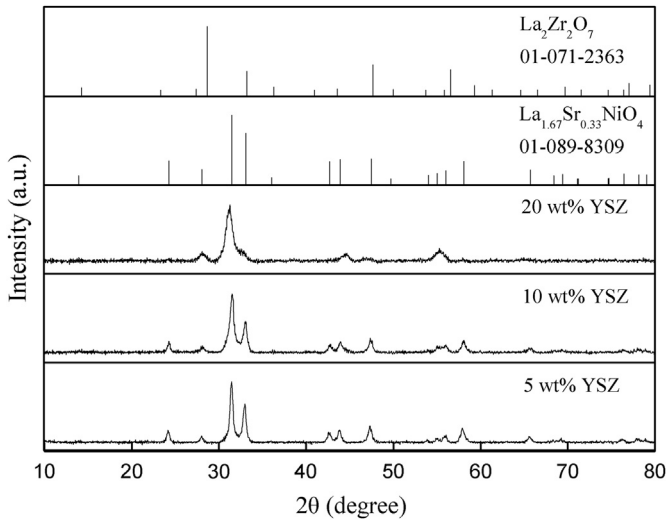

Fig. 3. XRD patterns for the samples of the powders after annealing at 800 °C for 2 h.

3.3. Sensor response

Fig. 5 shows the EMF response of the sensors with the different sensing electrodes to NO at 400–550 °C. The EMF values decrease with increasing operating temperature at a given gas concentration. The response becomes more rapid as temperature increases. At 400 °C (Fig. 4(d)), the EMF magnitude of the sensor fabricated with 10 wt% YSZ addition sensing electrode at 700 ppm of NO in 10% O_2 with N_2 balance is the largest (about 27 mV), while the EMF value of the sensor fabricated with 20 wt % YSZ addition sensing electrode at the same concentration is about 16.5 mV. The recovery of sensor fabricated with 20 wt% YSZ addition is also slower than the rest.

The response times and the recovery times are calculated from the transient potentiometric measurements by taking the times required for the voltages to reach 90% of their final steady-state values. At 400 °C, the sensor response is generally rapid, with a new steady-state attained within 30 s (Fig. 6(a)). The recovery times range from 6 to 71 s and are slower at higher NO concentrations (Fig. 6(b)). The sensor fabricated with 10 wt% YSZ addition has the fastest recovery of the samples tested.

Correlating these results with microstructures of the sensing electrodes (Fig. 4), when YSZ is added into sensing electrode, the superficial area of triple phase boundary (TPB) could be larger and electrode electrocatalytic activity could be enhanced, while maintaining adequate amount of reaction sites. But excessive YSZ (20 wt% addition) could form insulating pyrochlore phase ($La_2Zr_2O_7$), which is the main drawback for a sensing electrode.

4. Conclusions

$La_{1.67}Sr_{0.33}NiO_4$ and different concentration YSZ composites were successfully fabricated by the microwave-assisted complex-gel auto-combustion synthesis method. Citric acid played an important role as a chelating agent in the synthesis process. The sensor fabricated with 10 wt% YSZ addition sensing electrode had the highest sensitivity (about 27 mV of 700 ppm NO) with shorter response time (4–18 s) and recovery time (6–35 s). Because these composite particles had more reaction sites, e.g. the triple phase boundary (TPB) on adding yttria stabilized zirconia. However, when the composites contained 20 wt% YSZ, it could form insulating $La_2Zr_2O_7$ phase. The performance of the sensor fabricated with 20 wt% YSZ addition was worse than the others.

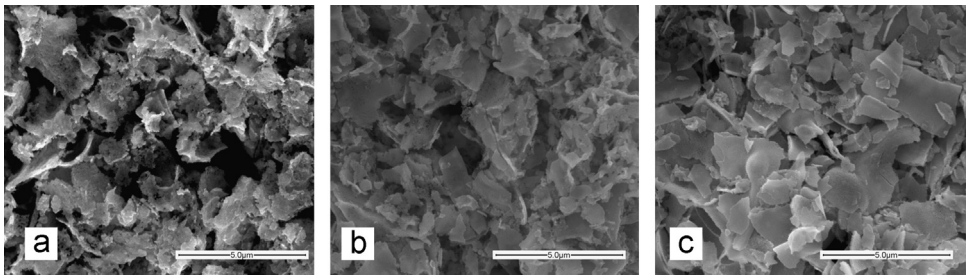

Fig. 4. ESEM surfaces of sensing electrodes: (a) $La_{1.67}Sr_{0.33}NiO_4$+5 wt% YSZ, (b) $La_{1.67}Sr_{0.33}NiO_4$+10 wt% YSZ, and (c) $La_{1.67}Sr_{0.33}NiO_4$+20 wt% YSZ.

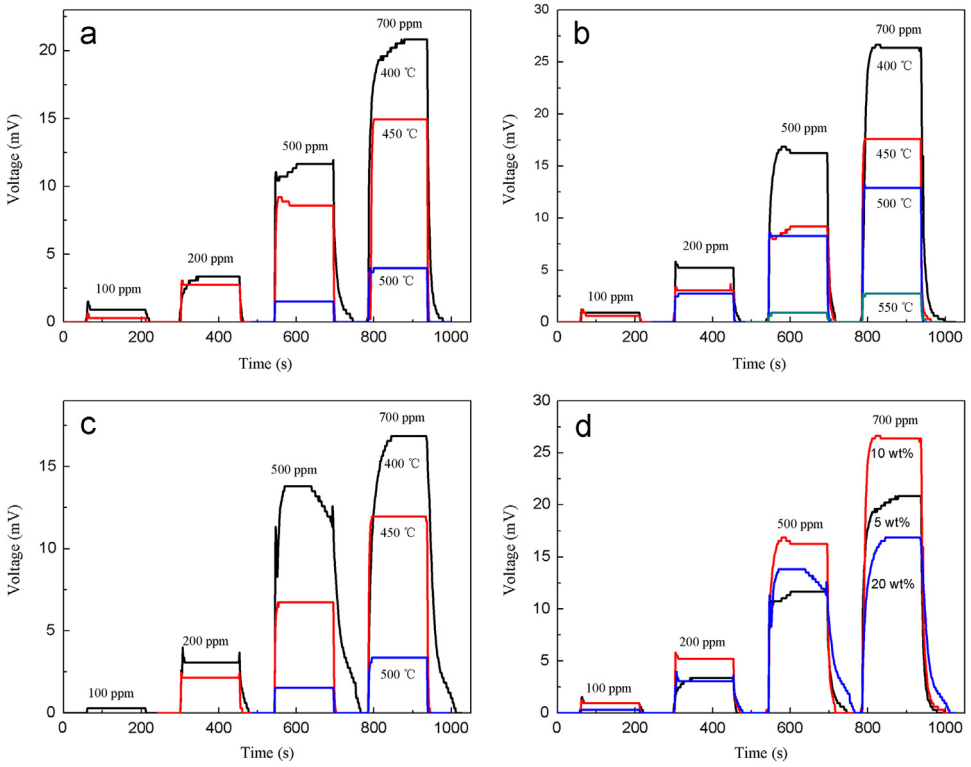

Fig. 5. (a)–(c) Sensor responses to step changes in NO concentration in 10% O_2 with N_2 balance at various temperatures. The sensors were fabricated with different sensing electrodes: (a) $La_{1.67}Sr_{0.33}NiO_4$+5 wt% YSZ, (b) $La_{1.67}Sr_{0.33}NiO_4$+10 wt% YSZ, (c) $La_{1.67}Sr_{0.33}NiO_4$+20 wt% YSZ; and (d) NO voltage response versus time of various sensing electrodes at 400 °C.

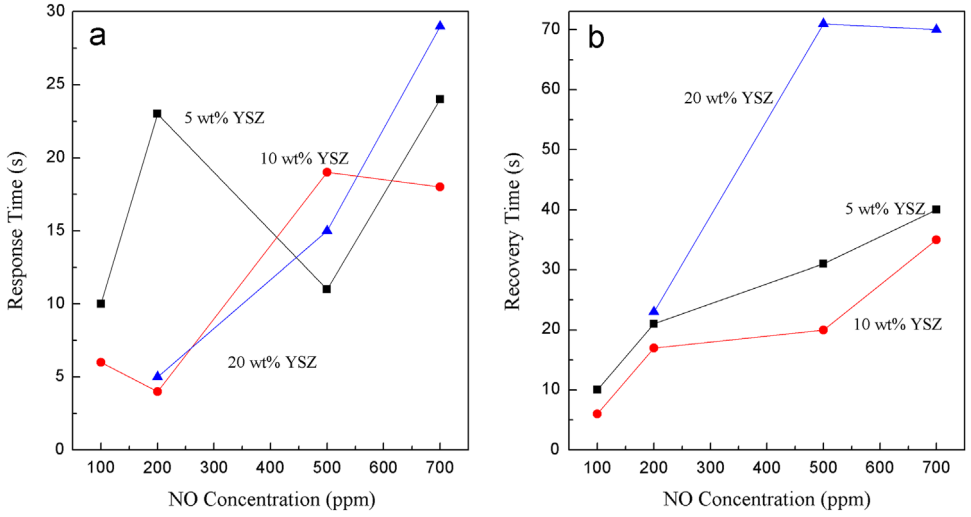

Fig. 6. Response time (a) and recovery time (b) at 400 °C of sensors fabricated with different sensing electrodes and sintered at 1000 °C for 2 h.

Acknowledgments

This research was supported by the National High Technology Research and Development Program of China (863 Program) under Contract NO. SS2012AA111716. The FTIR, XRD and SEM were conducted at the analytic and testing center of Huazhong University of Science and Technology.

References

[1] E.A. Efthimiadis, G.D. Lionta, S.C. Christoforou, I.A. Vasalos, The effect of CH_4, H_2O and SO_2 on the NO reduction with C_3H_6, Catalysis Today 40 (1998) 15–26.

[2] W. Schieber, H. Vinek, A. Jentys, Catalytic reduction of NOx over transition-metal-containing MCM-41, Catalysis Letters 56 (1998) 189–194.

[3] J.W. Fergus, Materials for high temperature electrochemical NOx gas sensors, Sensors and Actuators B: Chemical 121 (2007) 652–663.
[4] G. Lu, N. Miura, N. Yamazoe, High-temperature sensors for NO and NO_2 based on stabilized zirconia and spinel-type oxide electrodes, Journal of Materials Chemistry 8 (1997) 1445–1449.
[5] N. Miura, G. Lu, N. Yamazoe, High-temperature potentiometic/amperometric NOx sensors combining stabilized zirconia with mixed-metal oxide electrode, Sensors and Actuators B: Chemistry 52 (1998) 169–178.
[6] D.L. West, F.C. Montgomery, T.R. Armstrong, Electrode materials for mixed potential NOx sensors, Ceramic Engineering and Science Proceedings 3 (2004) 493–498.
[7] E. Boehm, J.M. Bassat, M.C. Steil, P. Dordor, F. Mauvy, J.C. Grenier, Oxygen transport properties of $La_2Ni_{1-x}Cu_xO_{4+\delta}$ mixed conducting oxides, Solid State Sciences 5 (2003) 973–981.
[8] L. Minervini, R.W. Grimes, J.A. Kilner, K.E. Sickafus, Oxygen migration in LaNiO, Journal of Materials Chemistry 10 (2000) 2349–2354.
[9] V.V. Kharton, A.P. Viskup, A.V. Kovalevsky, E.N. Naumovich, F.M. B. Marques, Ionic transport in oxygen-hyperstoichiometric phases with K_2NiF_4-type structure, Solid State Ionics 143 (2001) 337–353.
[10] E. Boehm, J.M. Bassat, P. Dordor, F. Mauvy, J.C. Grenier, P. Stevens, Oxygen diffusion and transport properties in non-stoichiometric $Ln_{2-x}NiO_{4+\delta}$ oxides, Solid State Ionics 176 (2005) 2717–2725.
[11] A.M. Daroukh, V.V. Vashook, H. Ullmann, F. Tietz, I. Arual Raj, Oxides of the AMO_3 and A_2MO_4-type: structural stability, electrical conductivity and thermal expansion, Solid State Ionics 158 (2003) 141–150.
[12] SJ Skinner, JA. Kilner, Oxygen diffusion and surface exchange in $La_{2-x}Sr_xNiO_{4+\delta}$, Solid State Ionics 135 (2000) 709–712.
[13] V.V. Vashook, N.E. Trofimenko, H. Ullmann, L.V. Makhnach, Oxygen nonstoichiometry and some transport properties of $LaSrNiO_{4-\delta}$ nickelate, Solid State Ionics 131 (2000) 329–336.
[14] J. Park, B.Y. Yoon, C.O. Park, W.J. Lee, C.B. Lee, Sensing behavior and mechanism of mixed potential NO sensors using NiO, NiO(+YSZ) and CuO oxide electrodes, Sensors and Actuators B: Chemistry 135 (2009) 516–523.
[15] Y.R. Hong, C.B. Gorman, Synthetic approaches to an isostructural series of redox-active, metal Tris(bipyridine) core dendrimers, ChemInform 35 (2004) 401–410.
[16] W.D. Yang, Y.H. Chang, S.H Huang, Influence of molar ratio of citric acid to metal ions on preparation of $La_{0.67}Sr_{0.33}MnO_3$ materials via polymerizable complex process, Journal of the European Ceramic Society 25 (2005) 3611–3618.
[17] S. Yan, W. Ling, E Zhou, Rapid synthesis of $Mn_{0.65}Zn_{0.35}Fe_2O_4SiO_2$ homogeneous nanocomposites by modified sol–gel auto-combustion method, Journal of Crystal Growth 273 (2004) 226–233.
[18] M. Matzapetakis, C.P. Raptopoulou, A. Terzis, A. Lakatos, T. Kiss, A. Salifoglou, Synthesis, structural characterization, and solution behavior of the first mononuclear, aqueous aluminum citrate complex, Inorganic Chemistry 38 (1999) 618–619.
[19] J. Liu, X. Fei, X. Yu, Z. Tao, L. Yang, S. Yang, Highly enhanced f–f transitions of Eu^{3+} in La_2O_3 phosphor via citric acid and poly(ethylene glycol) precursor route, Journal of Non-Crystalline Solids 353 (2007) 4697–4701.
[20] S. Musić, S. Popović, S. Dalipi, Formation of oxide phases in the system Fe_2O_3/NiO, Journal of Materials Science 28 (1993) 1793–1798.
[21] F. del Monte, W. Larsen, J.D. Mackenzie, Stabilization of tetragonal ZrO_2 in ZrO_2–SiO_2 binary oxides, Journal of the American Ceramic Society 83 (2000) 628–634.